

Design Optimization of QFP Structure for over 8Gbps Package Applications

Abstract. A 8Gbps packaging solution that uses low-cost quad flat pack (QFP) technology is presented. Since such a high speed is beyond the reach of traditional QFP package structure, a new design methodology with coplanar transmission line structure built into the lead frame has been developed. Due to the complexity level in QFP structure, each interconnect segment is accurately modelled in 3D model by utilizing the industry leading advance software tool, ANSYS HFSS. S-parameter, Time Domain Reflectometry (TDR) and Eye Diagram are used to help in understanding the contributing to the optimized QFP structure. The analysis results indicate that the optimized QFP structure can successfully achieve over 8Gbps single-end signal transmission.

Streszczenie. W artykule przedstawiono metodę zmiany struktury QFP na potrzeby przesyłu z prędkością 8Gbps. W celu analizy działania, stworzono model struktury o bardzo wysokiej precyzji, przy wykorzystaniu programów ANSYS HFSS. S-parameter, Time Domain Reflectometry (TDR) oraz Eye Diagram. Analiza wyników badań wykazuje, że wprowadzona optymalizacja pozwala na osiągnięcie założonej prędkości przesyłu danych. (Optymalizacja struktury QFP dla aplikacji o prędkości transmisji ponad 8Mbps).

Keywords: Quad flat package (QFP), electromagnetic modelling, lumped equivalent circuit model, coplanar transmission line structure.

Słowa kluczowe: QFP, modelowanie elektromagnetyczne, model układu o parametrach skupionych,

Introduction

Advances in fabrication technologies allow the speed (and frequency) of integrated circuits to increase rapidly. In order to reduce the gap between on-chip computational speed and off-chip communication bandwidth, some advanced packaging technologies such as flip-chip ball grid array package (FC-BGA), chip scale package (CSP), and ceramic package have been developed [1,2]. Compared with these advanced packaging techniques, lead frame plastic package technologies such as small outline packaging (SOP), shrink small outline packaging (SSOP), and miniature shrink small outline packaging (MSSOP) are still widely used to house high performance ICs because of their convenience and low cost. But these packages are smaller and fit for low pin count applications.

Quad Flat Pack (QFP) has been used for many years to house large scale or very large scale integrated circuits, but the use of QFP is limited to mid-speed and mid-frequency applications since parasitic parameters of bonding wires and leads significantly degrade the signal integrity at higher-speed (and higher-frequency). Fig. 1 illustrates the outline of a selected traditional QFP80 package. The dummy die is bonded to the paddle and encapsulated in plastic. Bond wires are used to provide connectivity from the die to the lead frame. In order to illustrate the parasitic effects, commercial electromagnetic analysis software HFSS is used to simulate the Z parameter of one set of signal path S1, S2 and S3 (donated by G-S-G), as shown in Fig. 1. Fig. 2 shows the EM simulated result when the signal S2 is shorted to ground through a bond wire. Z11 rises dramatically due to the internal inductive reactances and exhibits a very strong resonance at 3.8GHz, which makes the "short" appear as an open-circuit [3,4]. Clearly, QFP80 package is very difficult for circuits to work at these frequencies.

Several approaches for high-speed lead frame application have been made and reported during recent years, which have demonstrated 3.2Gbps differential signal transmission with LQFP256 for XDR memory controller [5,6]. However, it is very difficult to operate at such high speed with single-end signal transmission. Therefore, additional study is necessary to meet this demand. Despite the concerns of high frequency loss, we believe that the single-end signal transmission bandwidth of lead frame

package can be increased by further optimized design before relying on expensive packaging solutions.

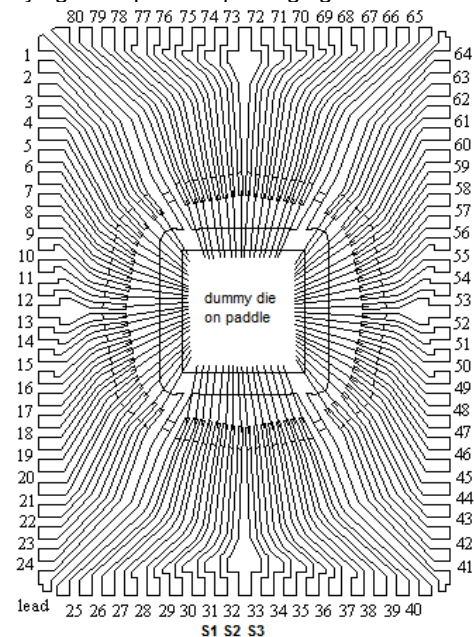


Fig. 1. Outline of a traditional QFP80 package

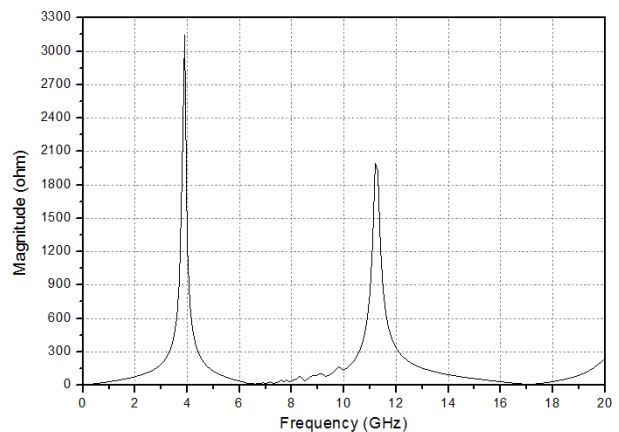


Fig. 2. Simulated result of Z11

In this paper, an optimized QFP80 package with coplanar transmission line structure has been developed. Each interconnect segment is accurately modelled in 3D model by HFSS. S-parameter, TDR and eye diagram are used to help in understanding the contributing to the optimized QFP80 structure. The analysis results show that the optimized model can achieve over 8Gbps single-end signal transmission.

Construction of the optimized QFP80 package

Usually, a traditional QFP80 lead frame can be modelled as a lumped equivalent circuit when the length of signal trace is less than one-tenth of work wavelength [7,8]. A cross-sectional view of the package and its corresponding equivalent circuit is given in Fig. 3. For simplicity, only three traces are selected. Leads and bond wires are modelled respectively. $L_{bondwire}$ and $R_{bondwire}$ are the lumped inductance and resistance of the bond wire. L_{lead} , R_{lead} and C_{lead} are the lumped inductance, resistance and capacitor of the lead. The terms $K_{bondwire}$ and K_{lead} are the magnetic coupling coefficients between the bond wires and the leads, respectively. There is also a capacitive coupling term C_{couple} between leads. This equivalent circuit neglects the coupling effects between lead S1 and lead S3, and between lead and bonding wire, because these coupling effects are much less than adjacent lead-to-lead and wire-to-wire. All these parasitic parameters of this lump equivalent circuit can be extracted by using quasi-static field simulator, such as ANSYS Q3D Extractor.

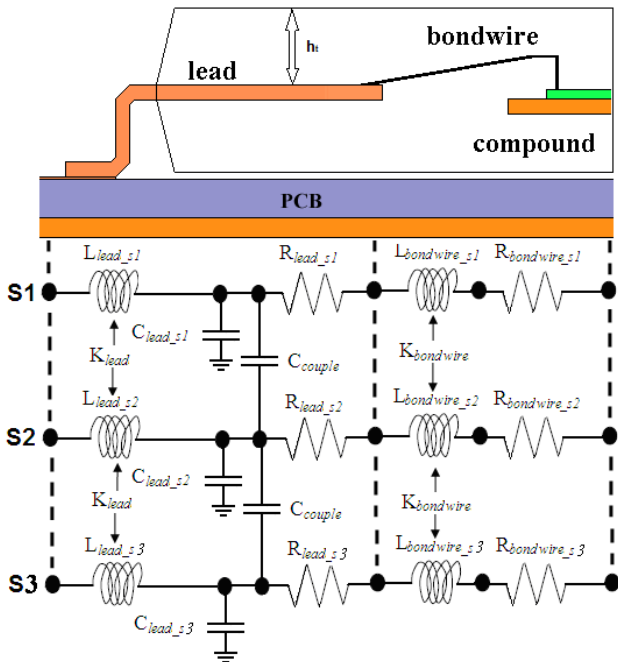


Fig.3. Simplified RLCM equivalent circuit of Lead Frame

In our work, we believe that if the QFP80 lead frame defined by characteristic impedance and electrical length may provide a better transmission performance than lumped elements mutually coupled to neighbouring traces. Fig. 4 shows a proposed transmission line equivalent circuit with the QFP80 lead frame designed as a coplanar transmission line. The raw coupling capacitance C_{couple} has been eliminated by tight coupling of the electric fields to the transmission line medium. Furthermore, the printed circuit board (PCB) transmission line can be effectively extended to the bond wire location. So, the purpose of optimal design is to make the discontinuity impedance of lead frame to be

close to the characteristic impedance of the PCB transmission line.

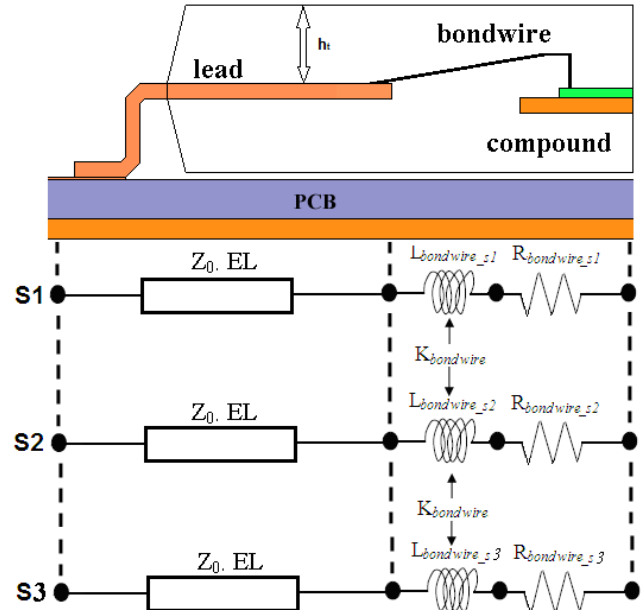


Fig.4. Transmission line equivalent circuit of Lead Frame

Fig. 5 illustrates the two cross-sectional views of the traditional S-S-S (or G-S-G) structure and proposed coplanar topology with finite irregular ground structure, respectively. As clearly seen, with both adjacent conductors S1 and S3 grounded, the three leads have been used to construct a coplanar transmission line structure, similar to that of a coplanar waveguide [9-11]. Two physical changes transform the QFP80 lead frame into coplanar transmission line structure. The first is that the grounded leads S1 and S3 have been extended to connect the paddle and the signal lead S2 has been extended to close the ground shield. This change not only can provide a better ground shield to control crosstalk, but also can short the bond wire to achieve a lower inductance. The second is to set the width of signal lead and the space between leads to constant value. This change can be used to provide impedance control for signal trace. It should be noticed that the outside part of the signal lead is embedded in air ($\epsilon_r \approx 1$), while the inside part is embedded in compound ($\epsilon_r = 3.3$). Therefore, the full lead should be designed as a cascade coplanar structure.

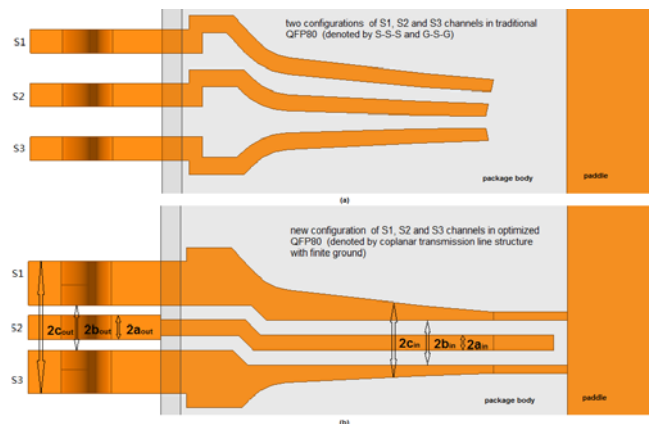


Fig.5. Two cross-sectional views: (a) traditional S-S-S or G-S-G structure and (b) proposed coplanar topology with finite irregular ground structure

In order to quantify the characteristic impedance of the coplanar transmission line structure, quasi-static analysis

can be adopted to extract the transmission line capacitances, which can be used to derive the effective dielectric constant ϵ_e and characteristic impedance Z_0 . The classic expressions of Z_0 and ϵ_e inside the package body are given as follows [12]:

$$(1) \quad Z_0 = \frac{1}{v\sqrt{\epsilon_e(C_{Ta}+C_{Ba}+C_{Pa})}}$$

$$(2) \quad \epsilon_e = \frac{C_{Ta}+C_{Td}+C_{Bd}+C_{Pd}}{C_{Ta}+C_{Ba}+C_{Pa}}$$

where: C_{Ta} – the per-unit-length capacitance produced by the top face of the leads without plastic dielectric (compound), C_{Td} – the per-unit-length capacitance produced by the top face of the leads with plastic dielectric, C_{Ba} – the per-unit-length capacitance produced by the bottom face of the leads without plastic dielectric, C_{Bd} – the per-unit-length capacitance produced by the bottom face of the leads with plastic dielectric, C_{Pa} – the per-unit-length capacitance produced by the parallel plate of the leads without plastic dielectric, C_{Pd} – the per-unit-length capacitance produced by the parallel plate of the leads with plastic dielectric, v – the speed of light in vacuum.

C_{Ta} and C_{Td} can be expressed as:

$$C_{Ta} = 2\epsilon_0 \frac{K \left(\frac{a_{in}}{b_{in}} \sqrt{\frac{1 - \frac{b_{in}^2}{c_{in}^2}}{1 - \frac{a_{in}^2}{c_{in}^2}}} \right)}{K' \left(\frac{a_{in}}{b_{in}} \sqrt{\frac{1 - \frac{b_{in}^2}{c_{in}^2}}{1 - \frac{a_{in}^2}{c_{in}^2}}} \right)}$$

and

$$C_{Td} = 2\epsilon_0(\epsilon_r - 1) \frac{K \left(\frac{\sinh(\frac{\pi a_{in}}{2h_t})}{\sinh(\frac{\pi b_{in}}{2h_t})} \sqrt{\frac{1 - \frac{\sinh^2(\frac{\pi b_{in}}{2h_t})}{\sinh^2(\frac{\pi c_{in}}{2h_t})}}{1 - \frac{\sinh^2(\frac{\pi a_{in}}{2h_t})}{\sinh^2(\frac{\pi c_{in}}{2h_t})}}} \right)}{K' \left(\frac{\sinh(\frac{\pi a_{in}}{2h_t})}{\sinh(\frac{\pi b_{in}}{2h_t})} \sqrt{\frac{1 - \frac{\sinh^2(\frac{\pi b_{in}}{2h_t})}{\sinh^2(\frac{\pi c_{in}}{2h_t})}}{1 - \frac{\sinh^2(\frac{\pi a_{in}}{2h_t})}{\sinh^2(\frac{\pi c_{in}}{2h_t})}}} \right)}$$

where: h_t , a_{in} , b_{in} , c_{in} – marked in Fig.4, Fig.5, ϵ_0 – the dielectric constant of vacuum, ϵ_r – the dielectric constant of compound, K , K' – the complete elliptic integrals and its complement.

The calculation of C_{Ba} and C_{Bd} are similar to the derivation of C_{Ta} and C_{Td} . Furthermore, C_{Pa} and C_{Pd} can be calculated by:

$$C_{Pa} = \frac{2\epsilon_0 t}{b_{in} - a_{in}}$$

and

$$C_{Pd} = C_{Pa} \times \epsilon_r$$

where: t – the thickness of lead.

The Z_0 and ϵ_e outside the package body can be obtained similarly.

Frequency domain analysis

The equation (1) and (2) derived from quasi-static analysis give us a good understanding for coplanar topology structure. However, the frequency dependent parameters for this structure are hard to quantify, and the discontinuity between the different segments is very complex especially at high frequency. So, ANSYS 3-D electromagnetic field solver HFSS, using finite element analysis, is adopted to simulate and analyze this coplanar structure.

In Fig. 6, the full traditional QFP80 package model including bond wires and leads is illustrated. Bonding wires are modelled based on the JEDEC standard. Two structures are simulated to investigate the impact of different circuit configurations based on the signal path S1, S2 and S3 (denoted by S-S-S and G-S-G, respectively). Each signal port is terminated to 50ohm. The setup of package material is stated in Table 1. Fig. 7 (a) and (b) show the simulated return loss (S11) and insertion loss (S21) of these two structures. In order to evaluate the applicable bandwidth for packaging structure easily, the insertion loss (S21) is compared at -1dB, and return loss (S11) is compared at -15dB. As shown in Fig. 7, the bandwidth measured for S11 is 1.2GHz (at -15dB, G-S-G structure), and 0.6GHz (at -15dB, S-S-S structure) respectively. Furthermore, the bandwidth of S21 is 2.3GHz (at -1dB, G-S-G structure), and 1.5GHz (at -1dB, S-S-S structure) respectively. It is obvious that the G-S-G structure shows better performance in traditional QFP80 package because the effective inductance is reduced and the effective capacitance is increased between the signal path and ground path.

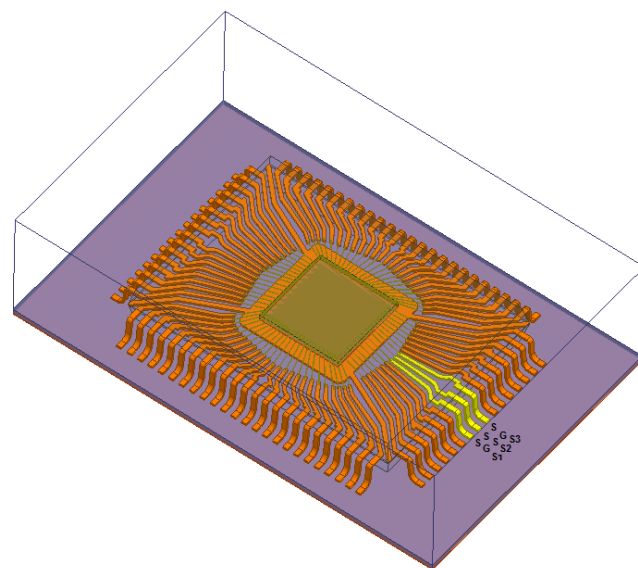


Fig.6. 3D model of the traditional QFP80 package

Table 1. Parameters of the traditional QFP80 package

Item	Description
Package body size	14×20×2.75mm ³ ($L \times W \times H$)
Lead width	0.35mm
Lead thickness	0.15mm
Bond wire diameter	0.025mm
Length of S1 path	Bond wire: 2.85mm Lead: 8.58mm
Length of S2 path	Bond wire: 2.8mm Lead: 8.32mm
Length of S3 path	Bond wire: 2.86mm Lead: 8.58mm
Material	Bond wire: gold, Lead: copper Compound: $\epsilon_r = 3.3$

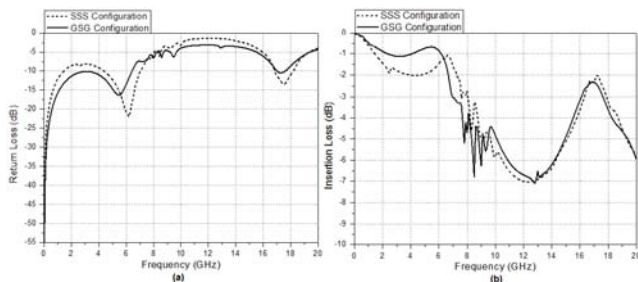


Fig.7. Simulated return loss (a) and insertion loss (b) of the S-S-S structure and G-S-G structure (including lead and bond wire)

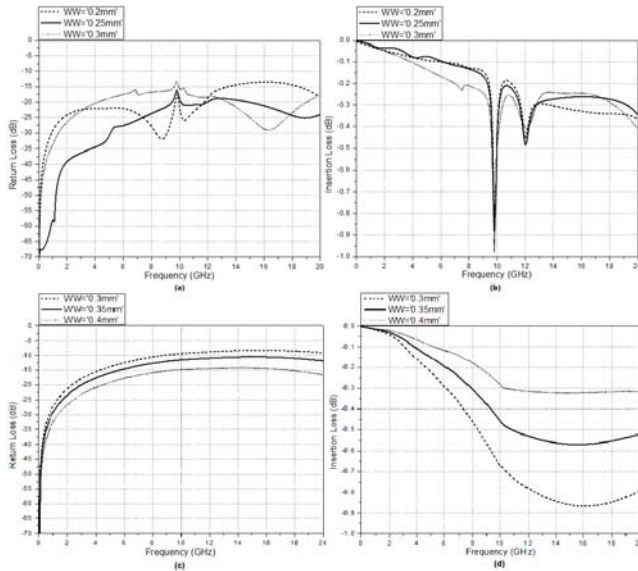


Fig.8. S-parameter sweep results: (a) return loss of inside part, (b) insertion loss of inside part, (c) return loss of outside part, and (d) insertion loss of outside part (lead only)

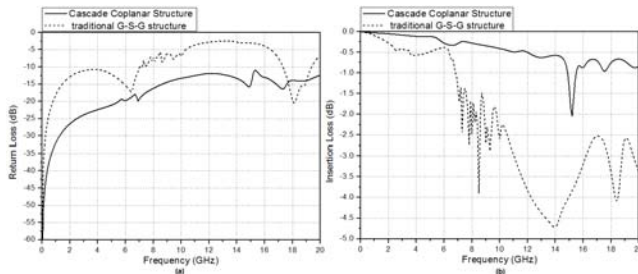


Fig.9. Simulated return loss (a) and insertion loss (b) of the proposed cascade transmission line structure and traditional G-S-G structure (lead only)

As mentioned before, the full coplanar transmission line structure should be designed as a cascade structure for more performance [13]. In order to match the characteristic impedance at the interface, the inside part and the outside part are modelled respectively. Six simulation configurations with different spacing and width are conducted to find a better compromise between performance, robustness and ease of fabrication, as shown in Table 2. Fig. 8 shows S-parameters from 10MHz to 20GHz for these configurations. From Fig. 8 (a) and (b), the scenario #2 shows better performance over the whole 20GHz bandwidth. Furthermore, from Fig. 8 (c) and (d), the scenario #6 with shortest distance between the signal lead and grounded lead is best for impedance matching. But the 0.130 mm spacing is difficult to fabricate. So, the proposed cascade structure can be constructed by combining scenario #2 and scenario #5. Fig. 9 shows the extensive simulation results of the proposed cascade coplanar transmission line

structure and the traditional G-S-G structure. As we can see, the cascade coplanar transmission line structure built into the lead frame is remarkable for discontinuity cancellation. This means that it is feasible to increase the bandwidth only by slight changes to the QFP80 lead frame before relying on expensive packaging solutions.

Table 2. Simulation configurations

Configuration	inside part of coplanar structure		outside part of coplanar structure	
	$2a_{in}$	$b_{in} - a_{in}$	$2a_{out}$	$b_{out} - a_{out}$
Scenario #1	0.20mm	0.230mm	-	-
Scenario #2	0.25mm	0.205mm	-	-
Scenario #3	0.30mm	0.180mm	-	-
Scenario #4	-	-	0.30mm	0.180mm
Scenario #5	-	-	0.35mm	0.155mm
Scenario #6	-	-	0.40mm	0.130mm

With the optimized coplanar transmission line structure built in, the final QFP80 3D model is given in Fig. 10. It should be noted that the traditional three leads (S1, S2 and S3) have been designed as the cascade coplanar structure. Fig. 11 (a) and (b) show the simulated return loss and insertion loss of the optimized structure and traditional G-S-G structure, the return loss (S11) is about -15dB (at 7.2GHz), and the insertion loss (S21) is about -1dB (at 9.5GHz). Compared with the traditional G-S-G model, the bandwidth of this optimized model measured for S11 and S21 is increased 500% and 317%, respectively.

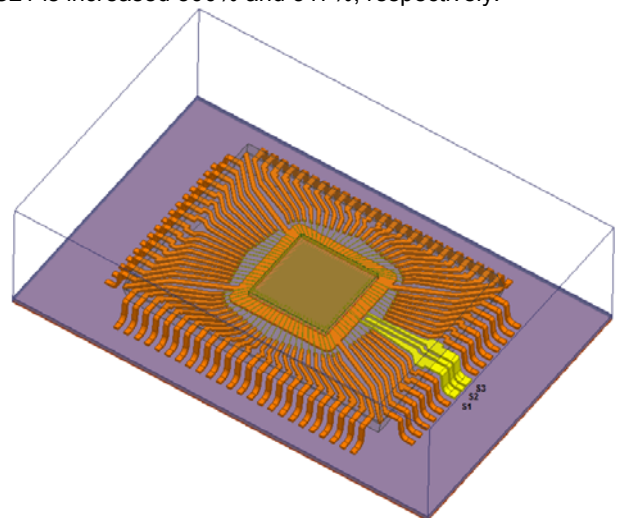


Fig.10. 3D model of the optimized QFP80 package with cascade coplanar transmission line structure built in

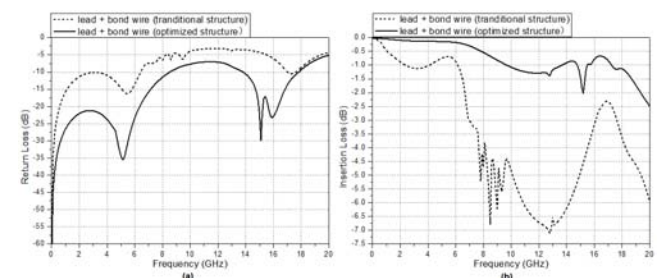


Fig.11. Simulated return loss (a) and insertion loss (b) of the optimized cascade transmission line structure and traditional G-S-G structure (including lead and bond wire)

In order to test the optimized QFP80 structure conveniently, a substrate with 50ohm microstrip line is fixed on the paddle, as shown in Fig. 12. Two optimized coplanar transmission line structures are constructed symmetrically. The shorter bond wires are used to connect the 50ohm microstrip line with these two coplanar structure. Other

leads are used for ground. The whole prototype has been fabricated and assembled on PCB with two SMA connectors for measurement. From Fig. 13 (a) and (b), we can see that the return loss and insertion loss follow the same trends over the whole 20GHz bandwidth and S21 show good agreement to 9GHz between the simulation and measurement. The frequency analysis results indicate the feasibility of our optimization design.

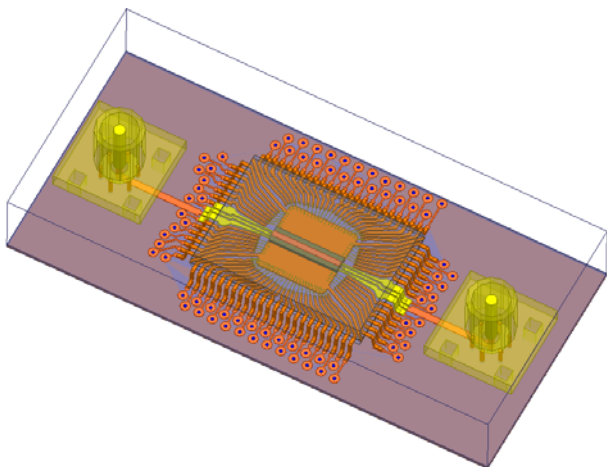


Fig.12. 3D model of the whole system for measurement

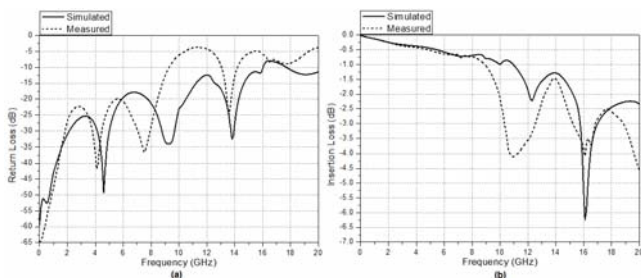


Fig.13. Measured and simulated return loss (a) and insertion loss (b) of the whole system

Time domain analysis

In order to evaluate the characteristic impedance, signal distortion and jitter of the optimized QFP80's ability intuitively, a time domain simulation would be necessary. TDR simulation allows us to overview the characteristic impedance of the whole package interconnect, and eye diagram gives us the ability to verify several performance characteristics, notably, deterministic jitter, as well as step responses[14-16].

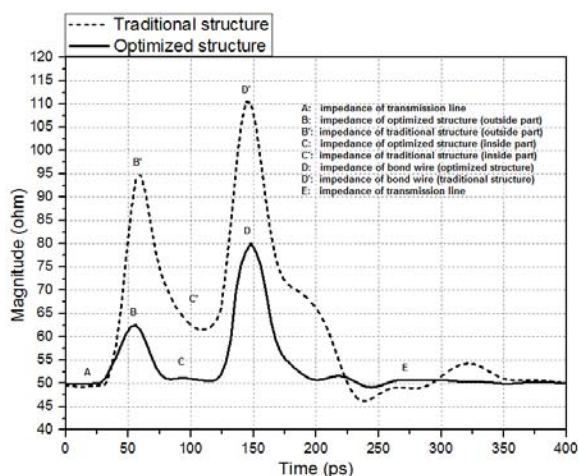


Fig.14. Simulated TDR results of the optimized cascade transmission line structure and traditional G-S-G structure

Fig. 14 shows the TDR simulation results for the optimized structure and the traditional structure. From the TDR plot, characteristic impedance of each segment can be captured clearly. The impedance of traditional lead segment has the maximum height of 95ohm (outside part) and the minimum height of 62 ohm (inside part), respectively. However, the impedance of optimized lead segment has the maximum height of 63 ohm and the minimum height of 51ohm, respectively. Furthermore, the impedance of the inductive wire bond has significantly reduced from 110ohm to 80ohm. It is obvious that the coplanar transmission line structure built in QFP80 is remarkable for impedance matching.

A pseudo-random binary source (PRBS) is used to do eye analysis and the simulated results are shown in Fig. 15. Compared with the traditional structure shown in Fig. 15 (a), It is clear that the eye formation of the optimized structure shown in Fig. 15 (b) is well intact, and very clean. The vertical eye opening of the optimized structure is 975mV, which is much better than 455mV of the traditional structure. Furthermore, from Fig. 15 (c) and (d), both 10Gbps and 12.5Gbps eye diagrams also show sufficient voltage and timing margins. The eye analysis results present a decisive demonstration that the coplanar transmission line structure built in QFP80 greatly improved the package bandwidth, achieving over 8Gbps data rate.

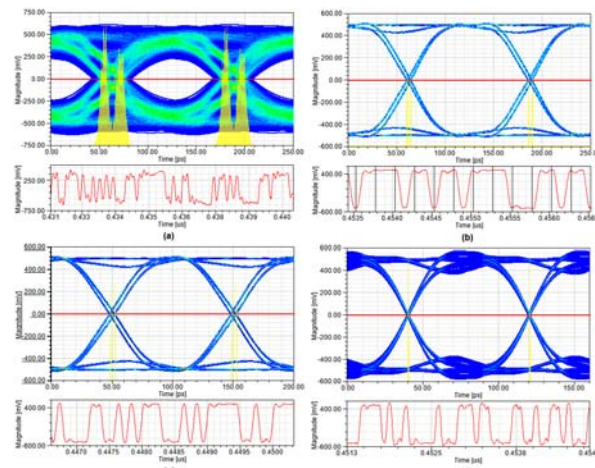


Fig.15. Eye diagram with histogram results: (a) 8Gbps eye of the traditional structure, (b) 8Gbps eye of the optimized structure, (c) 10Gbps eye of the optimized structure, and (d) 12.5Gbps eye of the optimized structure

Conclusions

In this paper, a cascade coplanar transmission line structure has been built in QFP80 package for high speed applications. Both traditional and optimized models have been constructed and analyzed in frequency and time domain. The analysis results indicate that the optimized QFP80 package is fully capable of supporting 8Gbps single-end signal transmission. Because this optimized structure needs layout space no more than traditional structure, it is suitable to be built in anywhere in QFP80 package. Additionally this design methodology could be readily applied not only the QFP80 package but also to any other lead frame packaging technologies.

Acknowledgments

The research work is financially supported by the Ministry of Industry and Information Technology of China (MIIT) (Grant No. 2009ZX01031-002-002), the National Natural Science Foundation of China (No.61040032) and the Educational Industrialization Foundation of Jiangsu Province (No. JHSD10-036).

REFERENCES

- [1] Hirose, T, "High-Frequency IC Packaging Technologies," *IEEE Indium Phosphide and Related Materials*, May. 2003, 227 - 230.
- [2] Tzyy-Sheng Horng; Sung-Mao Wu; Hui-Hsiang Huang; Chi-Tsung Chiu; Chih-Pin Hung, "Modeling of lead-frame plastic CSPs for accurate prediction of their low-pass filter effects on RFICs," *IEEE Transactions on Microwave Theory and Techniques*, Vol. 49, No. 9, 2001, 1538-1545.
- [3] Lawrence Larson, Darryl Jessie, "Advances in RF Packaging Technologies for Next-Generation Wireless Communications Applications", *IEEE Custom Integrated Circuits Conference*, 2003, 323-330
- [4] Haiyan Sun, Jianhui Wu, Ling Sun, Weiping Jing, "Optimization Design of a 64-Lead Low-Profile Quad Flat Package for RFIC Applications," *11th International Conference on Electronic Packaging Technology & High Density Packaging (ICEPT-HDP)*, August 2010, 499 – 502
- [5] Joong-Ho Kim, Ralf Schmitt, Dan Oh, Wendemagegnehu T. Beyene, Ming Li, Arun Vaidyanath, Yi Lu, June Feng, Chuck Yuan, Dave Secker, Don Mullen, "Design of Low Cost QFP Packages for Multi-Gigabit Memory Interface," *Electronic Components and Technology Conference*, 2009, 1662-1669
- [6] Joong-Ho Kim, Ralf Schmitt, Dan Oh, Wendemagegnehu T. Beyene, Ming Li, Arun Vaidyanath, June Feng, Chuck Yuan, "Feasibility Study of a 3.2Gb/s Memory Interface in Ultra Low-Cost LQFP Packages", *DesignCon 2009*, Santa Clara, 2009.
- [7] Darryl Jessie, Lawrence Larson, "An Improved Leaded Small Outline Package and Equivalent Circuit," *IEEE microwave and wireless components letters*, Vol. 13, No. 7, July 2003, 273-275
- [8] Umberto Paoletti, Takashi Hisakado, Osami Wada, "Quasi-Static Lumped Element Stand-Alone Package Model for Quad Flat Package," *Electrical Design of Advanced Packaging and Systems Symposium*, 2008, 57-60
- [9] J. Svacina, "A simple quasi-static determination of basic parameters of multilayer microstrip and coplanar waveguide," *IEEE Microwave and Guided Wave Letters*, Vol. 2, No. 10, pp. 382-387, October. 1992.
- [10] S. S. Bedair, I. Wolff, "Fast, accurate and simple approximate analytic formulas for calculating the parameters of supported coplanar waveguides for MMIC's," *IEEE Trans. on Microwave Theory and Techniques*, Vol. 40, No. 1, 1992, 41-48.
- [11] J. Ke, C. H. Chen, "Dispersion and attenuation characteristics of coplanar waveguides with finite metallization thickness and conductivity," *IEEE Trans. on Microwave Theory and Techniques*, Vol. 43, No. 5, 1995, 1128-1135.
- [12] D. Jessie, L. Larson, "Conformal mapping for buried CPW with finite grounds," *Electronics Letters*, Vol. 37, No. 25, December 2001, 1521-1523.
- [13] Haiyan Sun, Jianhui Wu, Ling Sun, Weiping Jing, "Modeling and Design of Coplanar Structure in QFP Package for RFIC Applications," *12th International Conference on Electronic Packaging Technology & High Density Packaging (ICEPT-HDP)*, August 2011, 573 – 576.
- [14] Beh Jiun Kai, Lee Chan Kim, "High Speed Interface Wirebond Modeling Division Methodology," *Electronic Materials and Packaging*, December 2006, 1-5.
- [15] Zhaowen YAN, Yansheng WANG, Mingming CHE, Yajing HAN, Tao WANG, Toyobur RAHMAN, "A Novel Design of Electromagnetic Bandgap Structure and its Effects on PI and SI," *Przegląd Elektrotechniczny*, No. 5, March 2012, 73-77.
- [16] Ryan D. McBride, Steven G. Rosser, and Ronald P. Nowak, "Modeling and Simulation of 12.5 Gbps on a HyperBGA Package," *Electronics Manufacturing Technology Symposium*, July 2003, 143-147.

Authors: Haiyan Sun, National ASIC System Engineering Research Center, Southeast University, Nanjing 210096, E-mail: sun.yan@seu.edu.cn; Zhikuang Cai, National ASIC System Engineering Research Center, Southeast University, Nanjing 210096, E-mail: whczk@seu.edu.cn; Jianhui Wu, Prof, National ASIC System Engineering Research Center, Southeast University, Nanjing 210096, E-mail: wjh@seu.edu.cn; Longxing Shi, Prof, National ASIC System Engineering Research Center, Southeast University, Nanjing 210096, E-mail: lxshi@seu.edu.cn; Ling Sun, Associate Prof, Jiangsu Provincial Key Lab of ASIC Design, Nantong University, Nantong 226019, E-mail: sun.l@ntu.edu.cn.